



Effect of CO on hydrogen storage performance of KF doped $2\text{LiNH}_2 + \text{MgH}_2$ material



Fei Sun, Min-yan Yan, Jian-hua Ye, Xiao-peng Liu*, Li-jun Jiang

Department of Energy Materials and Technology, General Research Institute for Non-Ferrous Metals, Beijing 100088, China

ARTICLE INFO

Article history:

Received 4 March 2014

Received in revised form 15 July 2014

Accepted 17 July 2014

Available online 24 July 2014

Keywords:

Hydrogen storage

Lithium–magnesium amide

CO impurity

Hydrogen capacity

Kinetics

ABSTRACT

$(2\text{LiNH}_2 + \text{MgH}_2)$ material is one of the most promising hydrogen storage materials. In applications, CO impurity in hydrogen has an effect on the hydrogen storage performance of $(2\text{LiNH}_2 + \text{MgH}_2)$ material. In this work, the effect of CO on the hydrogen storage properties of KF doped $(2\text{LiNH}_2 + \text{MgH}_2)$ material was investigated by using hydrogen containing 1 mol% CO as the hydrogenation gas source. The results indicate that the hydrogen desorption capacity of the hydride decreases from 4.73 wt.% to 3.88 wt.% after 5 hydrogenation cycles. The decrease of the capacity is attributed to the permanent loss of the NH_2 caused by the formation of Li_2CN_2 and KCN. Moreover, the hydrogen desorption kinetics declines obviously, and the dehydrogenation activation energy increases from 122.1 kJ/mol to 132.0 kJ/mol. Furthermore, it is found that the hydrogen desorption kinetics cannot be recovered to the initial level after re-milling. The main reason for these is that the catalytic effect on $(\text{Mg}(\text{NH}_2)_2 + 2\text{LiH} + 0.05\text{KF})$ system disappears due to the transformation from KH to KCN.

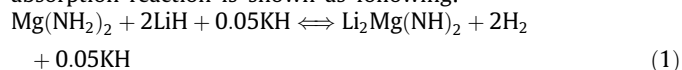
© 2014 Elsevier B.V. All rights reserved.

1. Introduction

The $(2\text{LiNH}_2 + \text{MgH}_2)$ material has been regarded as a potential hydrogen storage system due to its suitable operation temperature and high reversible hydrogen storage capacity of 5.6 wt.% among numerous of magnesium-based hydrides [1–10]. $(2\text{LiNH}_2 + \text{MgH}_2)$ transforms to $\text{Li}_2\text{Mg}(\text{NH})_2$ in the first hydrogen desorption process, and then it experiences the reversible process between $(\text{Li}_2\text{Mg}(\text{NH})_2 + 2\text{H}_2)$ and $(\text{Mg}(\text{NH}_2)_2 + 2\text{LiH})$ for the hydrogen absorption and desorption [3].

The theoretical dehydrogenation temperature of the $(\text{Mg}(\text{NH}_2)_2 + 2\text{LiH})$ is about 90 °C at 1.0 bar equilibrium hydrogen pressure [4]. However, the high operating temperature and low kinetics are still the main barriers for the practical application of the $(\text{Mg}(\text{NH}_2)_2 + 2\text{LiH})$ material. In the last decade, efforts have been focused on lowering the operating temperature and improving the kinetics of Li–Mg–N–H system [11–25]. Liu et al. [15] reported that the hydrogen storage performance of $(\text{Mg}(\text{NH}_2)_2 + 2\text{LiH})$ system was enhanced by introducing KF. It is found that KH, converted from KF, acted as a catalyst to decrease the activation energy of the first-step dehydrogenation, and meanwhile a reactant to reduce the desorption enthalpy change of the second step. This provides a synergetic thermodynamic and kinetic destabilization in the hydrogen storage

reaction of the $(\text{Mg}(\text{NH}_2)_2 + 2\text{LiH})$ system. Furthermore, the KF doped $(\text{Mg}(\text{NH}_2)_2 + 2\text{LiH})$ exhibits a good hydrogen storage reversibility. In this paper, the experimental material is referred to as $(2\text{LiNH}_2 + \text{MgH}_2 + 0.05\text{KF})$. The hydrogen desorption/absorption reaction is shown as following:



For practical application, hydrogen source contains reactive and inert impurities, such as CO, CO_2 , O_2 , H_2O , N_2 , and CH_4 . These impurities may have effects on the performance of hydrogen storage materials. The influence of the impurities on hydrogen storage alloys was widely investigated [26–38]. It was reported that the absorption kinetics of LaNi_5 and $\text{LaNi}_{4.73}\text{Sn}_{0.27}$ are strongly retarded by CO contamination [28]. However, thus far there has been little research on amides [39–42]. Luo and Ruckenstein [41] reported that water-saturated air could slightly improve the sorption kinetics and final hydrogen capacity. In the present work, hydrogen containing 1 mol% CO is employed as the hydrogenation gas source to study whether the hydrogen storage performance of the $(2\text{LiNH}_2 + \text{MgH}_2 + 0.05\text{KF})$ system is affected by CO impurity and how it works in practical application.

2. Experimental

The starting materials LiNH_2 (95% purity, Sigma–Aldrich) and KF (99% purity, Sigma–Aldrich), were used without further purification. The MgH_2 powder was prepared by mechanically milling Mg powder under an initial hydrogen pressure of

* Corresponding author. Tel.: +86 10 82241239.

E-mail address: xpqliu@126.com (X.-p. Liu).

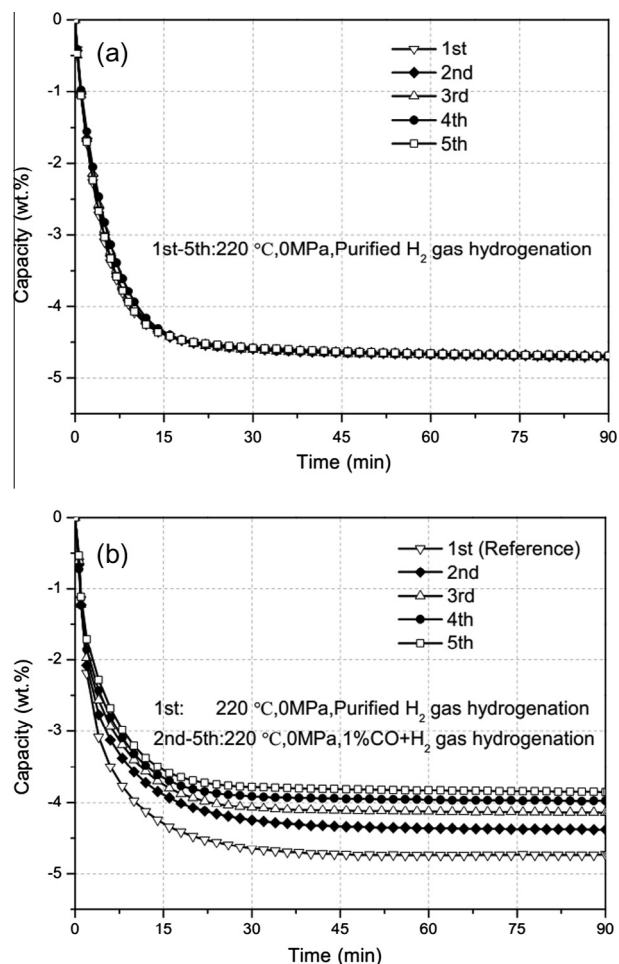


Fig. 1. Hydrogen desorption kinetics of the $(\text{Mg}(\text{NH}_2)_2 + 2\text{LiH} + \text{KF})$ mixture for (a) Sample 1 and (b) Sample 2 measured at 220 °C.

3 MPa for 40 h, followed by hydrogenation at 400 °C for 4 h under 8 MPa hydrogen pressure. A mixture of LiNH_2 , MgH_2 and KF with molar ratio of 2:1:0.05 was mechanically milled for 10 h under 3 MPa hydrogen pressure. All the milling treatment was done by using a Spex-8000 apparatus, and the ball-to-powder ratio was around 10:1. The material handling was performed in a glovebox filled with purified argon to keep the H_2O and O_2 levels below 1 ppm.

The hydrogen desorption kinetics measurements were carried on a Sieverts-type apparatus. The as-milled $(2\text{LiNH}_2 + \text{MgH}_2 + 0.05\text{KF})$ mixture yielded two samples (each weighs about 700 mg). Sample 1 was the reference group which experienced hydrogenation with purified H_2 for 5 cycles. Sample 2 was regarded as the experimental group which was firstly hydrogenated with purified H_2 , and then was hydrogenated with H_2 containing 1 mol% CO in the following 4 cycles. The initial pressures of dehydrogenation and hydrogenation were about 0 MPa and 8 MPa, and the end pressures were about 0.2 MPa and 7.9 MPa respectively. All the measurements were carried at 220 °C for 4 h.

Differential scanning calorimetry (DSC) was conducted by using Mettler-Toledo DSC 1 to study the dehydrogenation activation energy of the samples. The samples (about 18 mg for each) were heated from 30 °C to 350 °C at various heating rate, e.g., 1, 3, 5, 8 and 10 °C/min, under Ar gas (99.999%) with flow rate of 30 mL/min. XRD analysis was carried out by using X'pert Pro MPD diffractometer with $\text{Cu K}\alpha$ radiation at 40 kV and 40 mA over the range of 10–90°. The FTIR absorption spectrum of N–H and C–N was collected in diffuse reflectance infrared Fourier transform mode.

3. Results and discussion

3.1. Hydrogen desorption kinetics

Fig. 1 shows the hydrogen desorption kinetics of Sample 1 (**Fig. 1(a)**) and Sample 2 (**Fig. 1(b)**). It is seen from **Fig. 1(a)** that the hydrogen desorption curves change little from cycle 1 to cycle

5. Its reversible hydrogen storage capacity is more than 4.7 wt.%. In **Fig. 1(b)**, the down triangle represents the first desorption of the Sample 2 which is hydrogenated with purified H_2 , and the other symbols represent the desorption from the 2nd to 5th of Sample 2 which is hydrogenated with H_2 containing 1 mol% CO . During the first cycle, the sample releases 4.73 wt.% H_2 within 45 min. But when H_2 containing 1 mol% CO is employed as the hydrogenation source, the capacity declines obviously from the 2nd to 5th cycle. After 5 cycles, the hydrogen desorption capacity is only 3.88 wt.%. Moreover, the hydrogen desorption kinetics decreases obviously. It takes 6 min, 9 min, 11 min, 12 min and 14 min to release 3.5 wt.% H_2 from 1st to 5th cycles, respectively. Therefore, CO in hydrogen source obviously declines the hydrogen desorption capacity and kinetics of the $(\text{Mg}(\text{NH}_2)_2 + 2\text{LiH} + 0.05\text{KF})$ system.

3.2. Phase characterization

Figs. 2 and **3** show XRD patterns and FTIR spectra for the $(\text{Mg}(\text{NH}_2)_2 + 2\text{LiH} + 0.05\text{KF})$ mixture after hydrogenation (**Figs. 2(a)** and **3(a)**) and dehydrogenation (**Figs. 2(b)** and **3(b)**), respectively. In **Figs. 2** and **3**, upper lines represent patterns of Sample 1 which is hydrogenated with purified H_2 , and bottom lines stand for Sample 2 which has experienced 5 hydrogenation and dehydrogenation cycles with H_2 containing 1 mol% CO . It can be seen from **Fig. 2** that the main components for Sample 1 after hydrogenation are $\text{Mg}(\text{NH}_2)_2$, LiH and KH , and after dehydrogenation the main

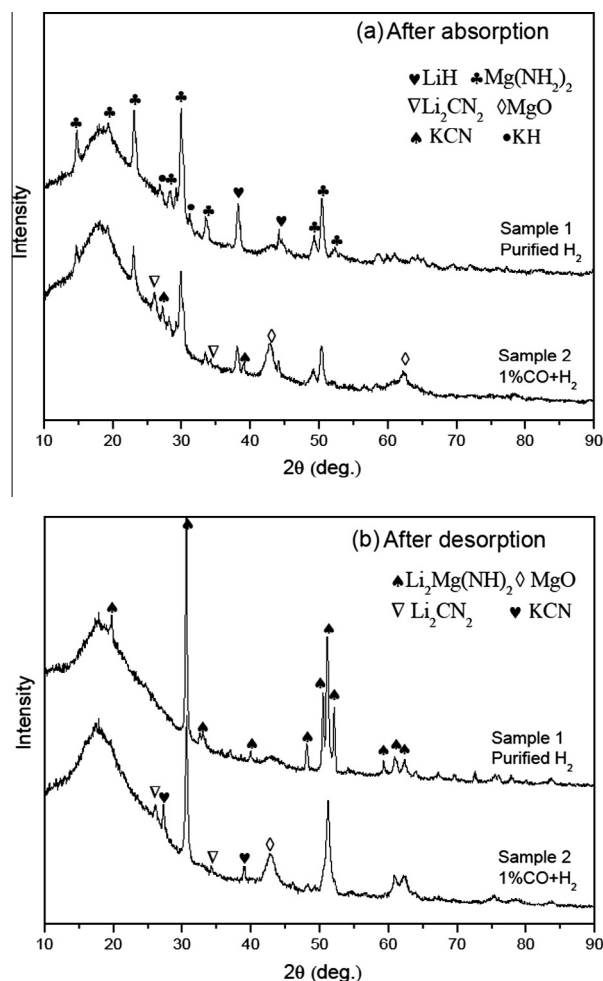


Fig. 2. Powder X-ray diffraction patterns of the $(\text{Mg}(\text{NH}_2)_2 + 2\text{LiH} + 0.05\text{KF})$ samples after (a) absorption and (b) desorption.

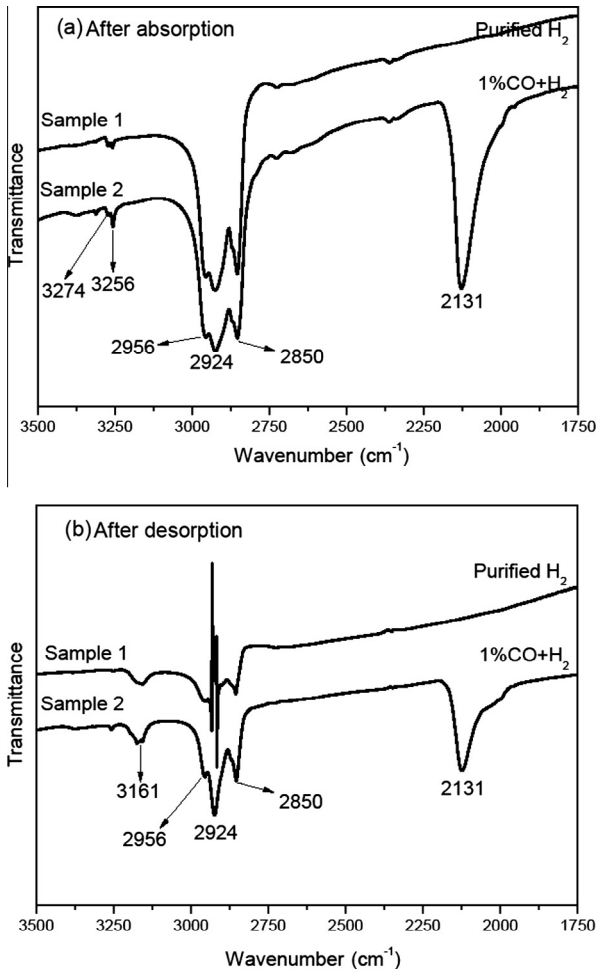
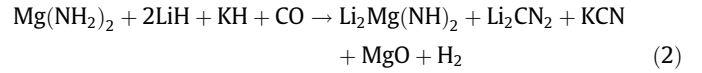


Fig. 3. FT-IR spectra of the $(\text{Mg}(\text{NH}_2)_2 + 2\text{LiH} + 0.05\text{KF})$ samples after (a) absorption and (b) desorption.

component is $\text{Li}_2\text{Mg}(\text{NH})_2$. After employing H_2 containing 1 mol% CO as the hydrogen source, KH disappears, and peaks of Li_2CN_2 , KCN and MgO appear.

One can see from FTIR spectra that the absorbance around 3200 cm^{-1} suggests the existence of N–H, and the peaks around 2900 cm^{-1} are attributed to Nujol oil. Compared with Sample 1, an absorbance peak at 2131 cm^{-1} attributed to the C–N vibration appears in Sample 2.

The XRD and FTIR analysis suggest that a bond break in CO occurs during hydrogenation when H_2 containing 1 mol% CO is employed as the hydrogen source. Then the carbon reacts with Li^+ , K^+ and N^{3-} to form Li_2CN_2 and KCN. And the oxygen reacts with Mg^{2+} to form MgO. The reaction is shown as following:



The reaction is irreversible because the new products of Li_2CN_2 , KCN and MgO are found in hydrogenation and dehydrogenation products. It is well known that nitrogen in NH_2^- or $(\text{NH}_2)^-$ plays a key role in Li–Mg–N–H system, because the conversion between NH_2^- and $(\text{NH}_2)^-$ is the main reaction process during hydrogenation and dehydrogenation. So the permanent loss of nitrogen results in the decline of hydrogen storage capacity.

3.3. Dehydrogenation activation energy

To understand the decline of the dehydrogenation kinetics more deeply, differential scanning calorimetry (DSC) was conducted to study the dehydrogenation activation energy of samples. Fig. 4 shows the DSC profiles for Sample 1 and Sample 2 after 5 hydrogenation and dehydrogenation cycles. Two Kissinger plots were drawn to estimate the activation energies. For Sample 2, the overall peak positions shift to the right direction of $45\text{--}50\text{ }^\circ\text{C}$ compared to those of Sample 1. According to Kissinger theory [43], the activation energies of hydrogen desorption are 122.1 kJ/mol and 132.0 kJ/mol for Samples 1 and 2, respectively. The activation energy increases 8% for the sample after hydrogenated with hydrogen containing 1 mol% CO, resulting in the decline of hydrogen desorption kinetics of the $(\text{Mg}(\text{NH}_2)_2 + 2\text{LiH} + 0.05\text{KF})$ sample.

There are two possible reasons for the decrease of the hydrogen desorption kinetics. One is that the new products of Li_2CN_2 , KCN and MgO formed on the surface of material particles prevent substance transmission during the dehydrogenation process. The

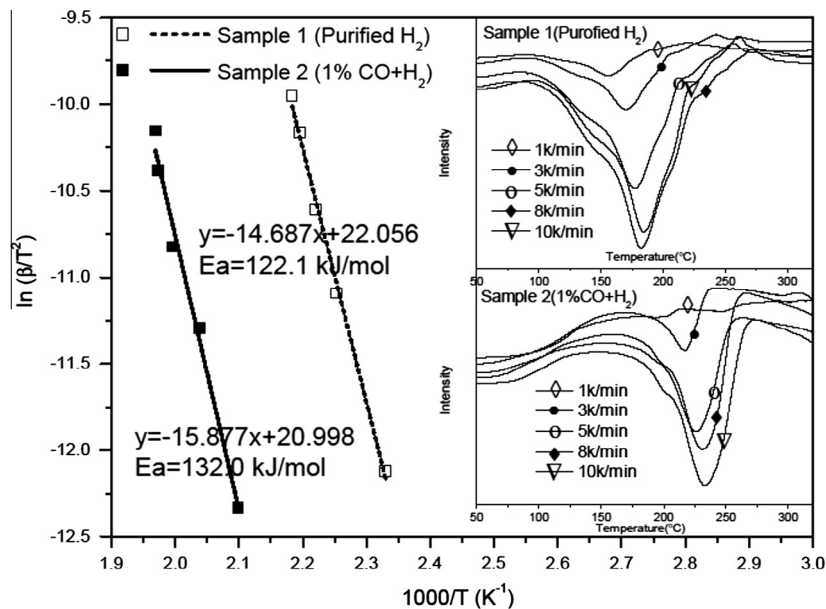


Fig. 4. Kissinger plots and DSC curves of the $(\text{Mg}(\text{NH}_2)_2 + 2\text{LiH} + 0.05\text{KF})$ samples.

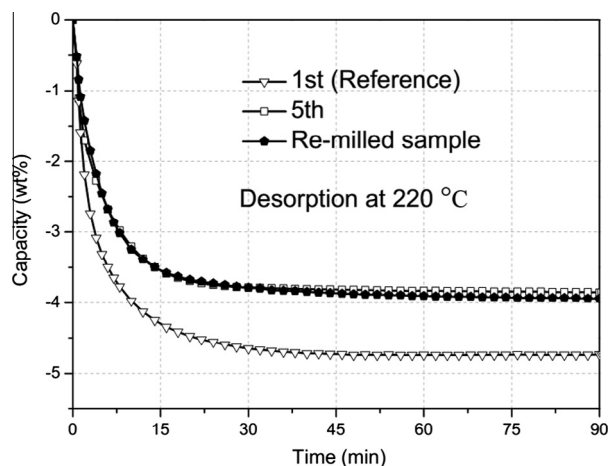


Fig. 5. Hydrogen desorption kinetics of there-milled sample measured at 220 °C.

other is that the catalytic effect on $(\text{Mg}(\text{NH}_2)_2 + 2\text{LiH} + 0.05\text{KF})$ system disappears due to the transformation from KH to KCN.

Verification experiment was done to find the main reason for the decrease of the hydrogen desorption kinetics. Sample 2, which has experienced 5 hydrogenation cycles with H_2 containing 1 mol% CO, was re-milled for 10 h to study whether the hydrogen desorption kinetics can be recovered. If it is recovered, the main reason is the slow substance transmission in dehydrogenation. Because the re-milling treatment can break the coating of the new products formed on the surface of material particles, providing the effective channels for the substance transmission. If not, the main reason is that the catalytic effect of KH disappears. Fig. 5 shows hydrogen desorption kinetics of the re-milled Sample 2. The data of the 1st and 5th desorption was collected from Fig. 1(b). It can be seen that the hydrogen desorption kinetics of the re-milled sample cannot be restored to the initial level. So it is suggested that the disappearance of the catalytic effect of KH due to the transformation from KH to KCN is the main reason for the decline of hydrogen desorption kinetics of the $(\text{Mg}(\text{NH}_2)_2 + 2\text{LiH} + 0.05\text{KF})$ material.

4. Conclusions

When H_2 containing 1 mol% CO is employed as the hydrogen source for $(\text{Mg}(\text{NH}_2)_2 + 2\text{LiH} + 0.05\text{KF})$ system, three new stable phases, Li_2CN_2 , KCN and MgO are formed. The reversible hydrogen desorption capacity gradually declines due to the permanent loss of NH_2^- in the hydride. Moreover, the hydrogen desorption kinetics decreases and the dehydrogenation activation energy increases obviously, because of the disappearance of the catalytic effect of KH due to the transformation from KH to KCN.

Acknowledgment

The authors would like to acknowledge the financial supports from National Basic Research Program of China (Grant No.

2010CB631305) under the Ministry of Science and Technology of China.

References

- [1] Z. Xiong, G. Wu, J. Hu, P. Chen, J. Adv. Mater. 16 (2004) 1522–1525.
- [2] W. Luo, J. Alloys Comp 381 (2004) 284–287.
- [3] W. Luo, E. Rönnebro, J. Alloys Comp. 404–406 (2005) 392–395.
- [4] Z. Xiong, J. Hu, G. Wu, P. Chen, W. Luo, K. Gross, J. Wang, J. Alloys Comp. 398 (2005) 235–239.
- [5] L. Ouyang, X. Yang, H. Dong, M. Zhu, Scr. Mater. 61 (2009) 339–342.
- [6] L. Ouyang, S. Ye, H. Dong, M. Zhu, Appl. Phys. Lett. 90 (2007) 021917.
- [7] M. Zhu, H. Wang, L. Ouyang, M. Zeng, Int. J. Hydrogen Energy 31 (2006) 251–257.
- [8] M. Zhu, Y. Gao, X. Che, Y. Yang, C. Chung, J. Alloys Comp. 708 (2002) 330–332.
- [9] G. Liu, Y. Wang, L. Jiao, H. Yuan, Int. J. Hydrogen Energy 39 (2014) 3822–3829.
- [10] G. Liu, F. Qiu, J. Li, Y. Wang, L. Li, C. Yan, L. Jiao, H. Yuan, Int. J. Hydrogen Energy 37 (2012) 17111–17117.
- [11] C. Liang, Y. Liu, M. Gao, H. Pan, J. Mater. Chem. A 1 (2013) 5031–5036.
- [12] T. Durojaiye, A. Coudy, Int. J. Hydrogen Energy 37 (2012) 3298–3304.
- [13] A. Sudik, J. Yang, D. Halliday, C. Wolverton, J. Phys. Chem. C 111 (2007) 6568–6573.
- [14] J. Hu, Y. Liu, G. Wu, Z. Xiong, Y.S. Chua, P. Chen, J. Chem. Mater. 20 (2008) 4398–4402.
- [15] Y. Liu, C. Li, B. Li, M. Gao, H. Pan, J. Phys. Chem. C 117 (2013) 866–875.
- [16] J. Wang, T. Liu, G. Wu, W. Li, Y. Liu, C. Moyses Araujo, R.H. Scheicher, A. Bomqvist, R. Ahuja, Z. Xiong, P. Yang, M. Gao, H. Pan, P. Chen, Angew. Chem. Int. Ed. 48 (2009) 5828–5832.
- [17] C. Liang, Y. Liu, H. Fu, Y. Ding, M. Gao, H. Pan, J. Alloys Comp. 509 (2011) 7844–7853.
- [18] C. Li, Y. Liu, Y. Pang, M. Gu, M. Gao, H. Pan, Dalton Trans. 43 (2014) 2369–2377.
- [19] B. Li, Y. Liu, J. Gu, Y. Gu, M. Gao, H. Pan, Int. J. Hydrogen Energy 38 (2013) 5030–5038.
- [20] Y. Liu, K. Zhong, K. Luo, M. Gao, H. Pan, Q. Wang, J. Am. Chem. Soc. 131 (2009) 1862–1870.
- [21] C. Li, Y. Liu, Y. Gu, M. Gao, H. Pan, Chem. Asian J. 8 (2013) 2136–2143.
- [22] B. Li, Y. Liu, C. Li, M. Gao, H. Pan, J. Mater. Chem. A 2 (2014) 3155–3162.
- [23] H. Pan, S. Shi, Y. Liu, B. Li, Y. Yang, M. Gao, Dalton Trans. 42 (2013) 3802–3811.
- [24] B. Li, Y. Liu, J. Gu, M. Gao, H. Pan, Chem. Asian J. 8 (2013) 374–384.
- [25] M. Yan, F. Sun, X. Liu, J. Ye, H. Yuan, S. Wang, L. Jiang, J. Alloys Comp. 603 (2014) 19–22.
- [26] T. Zhang, X. Yang, J. Li, R. Hu, X. Xue, H. Fu, J. Power Sources 202 (2012) 217–224.
- [27] F.G. Eisemoerg, P.D. Goodell, J. Less-common Met. 89 (1983) 55–62.
- [28] E.M. Borzone, M.V. Blanco, G.O. Meyer, A. Baruj, Int. J. Hydrogen Energy 39 (2014) 10517–10524.
- [29] D. Dunikov, V. Borzenko, S. Malyschenko, Int. J. Hydrogen Energy 37 (2012) 13843–13848.
- [30] K.D. Modibane, M. Williams, M. Lototsky, M.W. Davids, Ye. Klochko, B.G. Pollet, Int. J. Hydrogen Energy 38 (2013) 9800–9810.
- [31] M. Lototsky, K.D. Modibane, M. Williams, Ye. Klochko, V. Linkov, B.G. Pollet, J. Alloys Comp. 580 (2013) S382–S385.
- [32] H. Lin, K. Lin, C. Sung, K. Wu, Int. J. Hydrogen Energy 32 (2007) 2494–2500.
- [33] F. Schweppe, M. Martin, E. Fromm, J. Alloys Comp. 253–254 (1997) 511–514.
- [34] J. Han, J. Lee, J. Less-common Met. 152 (1989) 319–327.
- [35] J. Han, J. Lee, J. Less-common Met. 152 (1989) 329–338.
- [36] D.M. Gualtieri, K. Narasimhan, T. Takeshita, J. Appl. Phys. 47 (1976) 3432–3435.
- [37] S. Myhra, E.H. Kisi, E.M. Gray, J. Alloys Comp. 224 (1995) 305–315.
- [38] J.I. Han, L.J. Young, J. Less-common Met. 157 (1990) 187–199.
- [39] Y. Hu, E. Ruckenstein, Ind. Eng. Chem. Res. 46 (2007) 5940–5942.
- [40] Y. Hu, E. Ruckenstein, Ind. Eng. Chem. Res. 47 (2008) 48–50.
- [41] S. Luo, T.B. Flanagan, W. Luo, J. Alloys Comp. 440 (2007) L13–L17.
- [42] F. Sun, M. Yan, X. Liu, J. Ye, Z. Li, S. Wang, L. Jiang, Int. J. Hydrogen Energy 39 (2014) 9288–9292.
- [43] E. Homer, Anal. Chem. 29 (1957) 1702–1706.